

Lense-Thirring Precession and QPOs in X-Ray Binaries

Dragoljub Marković and Frederick K. Lamb¹

*University of Illinois at Urbana-Champaign, Department of Physics
1110 W. Green Street, Urbana, IL 61801, USA*

ABSTRACT

It has recently been suggested that gravitomagnetic precession of the inner part of the accretion disk, possibly driven by radiation torques, may be responsible for some of the quasi-periodic X-ray brightness oscillations (QPOs) and other spectral features with frequencies between 20 and 300 Hz observed in the power spectra of some low-mass binary systems containing accreting neutron stars and black hole candidates. We have explored the free and driven normal modes of geometrically thin disks in the presence of gravitomagnetic and radiation warping torques.

We have found a family of low-frequency gravitomagnetic (LFGM) modes with precession frequencies that range from the lowest frequency allowed by the size of the disk up to a certain critical frequency ω_{crit} , which is ~ 1 Hz for a compact object of solar mass. The lowest-frequency (lowest-order) LFGM modes are similar to the previously known radiation warping modes, extend over much of the disk, and have damping rates $\gtrsim 10$ times their precession frequencies. The highest-frequency LFGM modes are tightly wound spiral corrugations of the disk that extend to ~ 10 times its inner radius and have damping rates $\gtrsim 10^3$ times their precession frequencies. A radiation warping torque can cause a few of the lowest-frequency LFGM modes to grow with time, but even a strong radiation warping torque has essentially no effect on the LFGM modes with frequencies $\gtrsim 10^{-4}$ Hz.

We have also discovered a second family of high-frequency gravitomagnetic (HFGM) modes with precession frequencies that range from ω_{crit} up to slightly less than the gravitomagnetic precession frequency $\omega_{\text{gm},i}$ of a particle at the inner edge of the disk, which is 30 Hz if the disk extends inward to the innermost stable circular orbit around a $2M_{\odot}$ compact object with dimensionless angular momentum $cJ/GM^2 = 0.2$. The lowest-frequency HFGM modes are very strongly damped and have warp functions and precession frequencies very similar to those of the highest-frequency LFGM modes. In contrast, the highest-frequency (lowest-order) HFGM modes are very localized spiral corrugations of the inner disk and are weakly damped, with Q values ~ 2 –50.

We discuss the implications of our results for the observability of Lense-Thirring precession in X-ray binaries.

Subject headings: accretion disks — black hole physics — gravitation — relativity — stars: neutron

¹Also, Department of Astronomy, University of Illinois at Urbana-Champaign.

1. INTRODUCTION

The possibility of observing gravitomagnetic (Lense-Thirring) precession of accretion disks around compact objects was considered early in the study of accretion onto black holes and neutron stars. The conclusion reached then (Bardeen & Petterson 1975; see also Petterson 1977a, 1977b, 1978; Hatchett, Begelman, & Sarazin 1981) was that the combined action of gravitomagnetic and internal viscous torques forces the disk flow into the rotation equator of the compact object at ~ 100 gravitational radii and holds it there, if the outer disk is misaligned or the disk is driven by time-independent torques. As a result, it has been widely thought that gravitomagnetic precession of the inner disk is unpromising as an explanation for X-ray oscillations.

Recently Ipser (1996) has investigated ‘trapped’ (i.e., localized; see Kato & Honma 1991) pressure perturbations that warp the innermost parts of accretion disks, found that the frame dragging near a Kerr black hole causes precession of such perturbations, and discussed their possible relation to the low-frequency quasi-periodic oscillations (QPOs) observed in the X-ray brightness of black hole candidates (see van der Klis 1995). The existence of these modes depends on the presence of specific (but not implausible) non-Keplerian angular velocity profiles. Ipser’s general relativistic analysis did not take into account the viscosity of the gas in the disk.

More recently, Stella & Vietri (1998) have suggested that gravitomagnetic precession of the inner disk may be responsible for the broad bumps that are observed between 20 and 60 Hz in the power spectra of some of the accreting neutron stars in low-mass binary systems called atoll sources and for the ~ 15 –65 Hz horizontal branch quasi-periodic oscillation (QPO) observed in the X-ray brightness of the so-called Z sources (see van der Klis 1995). It has been conjectured (e.g., Stella 1997a, 1997b) that the tilt of the inner disk required for gravitomagnetic precession could be caused either by the radiation torque thought to produce radiation warping of accretion disks (see Iping & Petterson 1990; Pringle 1996; Maloney, Begelman, & Pringle 1996; Maloney & Begelman 1997) or by forcing of the inner disk by the neutron star’s magnetic field. Cui, Zhang, & Chen (1998) subsequently suggested that the ~ 6 –300 Hz QPOs observed in the X-ray brightness of the galactic black hole candidates (Miyamoto et al. 1991; Morgan,

Remillard, & Greiner 1997; Remillard 1997) may be produced by gravitomagnetic precession. These suggestions have renewed interest in the possibility of observing gravitomagnetic precession near compact objects.

In this paper we report calculations of the properties of gravitomagnetic and radiation warping modes of geometrically thin, Keplerian α disks. Our work goes beyond previous work in several ways. First, we have computed the radiation warping mode functions and their frequencies and growth rates up to very high mode numbers. Our results for the tilt functions and precession frequencies of the low-order radiation warping modes agree well with previous results (Maloney et al. 1996). Second, we have explored the time-dependent gravitomagnetic modes of the disk, including both undriven (free) modes and modes that are being driven at the inner boundary. Third, we have investigated the combined effects of gravitomagnetic and radiation torques. Finally, we have considered not only isothermal disks but also disks with a variety of radial temperature structures, and inner and outer boundary conditions appropriate to a variety of astrophysical situations.

We have found a family of low-frequency gravitomagnetic (LFGM) modes with precession frequencies that range from the lowest frequency allowed by the size of the disk up to a certain critical frequency ω_{crit} , which is ~ 1 Hz for a compact object of solar mass. The lowest-order (fundamental) LFGM mode is the zero-frequency mode found earlier by Bardeen & Petterson (1975). The other low-order LFGM modes are long-wavelength, precessing corrugations of the outer disk similar to the previously known low-order radiation warping modes and have damping rates $\gtrsim 10$ times their precession frequencies. The highest-frequency LFGM modes are very tightly wound spiral corrugations of the inner disk that extend only to ~ 10 times the inner radius of the disk and have damping rates $\gtrsim 10^3$ times their precession frequencies. A radiation warping torque makes all the low-order modes in this family time-dependent and can cause a few of the lowest-frequency LFGM modes to grow with time, but even a strong radiation warping torque has essentially no effect on the modes with frequencies $\gtrsim 10^{-4}$ Hz.

We have also discovered a second family of high-frequency gravitomagnetic (HFGM) modes with precession frequencies that range from ω_{crit} up to slightly less than the gravitomagnetic precession frequency

$\omega_{\text{gm},i}$ of a particle at the inner edge of the disk. The highest possible mode frequency is the gravitomagnetic precession frequency at the innermost stable circular orbit, which is 30 Hz for a $2M_{\odot}$ compact object with dimensionless angular momentum $cJ/GM^2 = 0.2$. The dozen highest-frequency (lowest-order) HFGM modes are very localized spiral corrugations of the inner disk, have precession frequencies that differ by a factor of two, and are weakly damped, with Q values ~ 2 -50. The lowest-frequency HFGM modes have shapes very similar to the highest-frequency LFGM modes and are very strongly damped.

The ‘trapped’ precessing modes discussed by Ipser (1996; see also references therein) and the HFGM modes discussed here are both localized near the inner edge of the disk, but unlike the trapped modes, the HFGM modes do not require rotation or epicyclic frequency profiles with any special shape. In fact, the shapes, precession frequencies, and damping rates of the modes in both the families we have studied depend only weakly on whether the gravitational potential used is the $1/r$ Newtonian potential or one of several pseudopotentials designed to mimic the steeper effective gravitational potentials of general relativity (see, e.g. Nowak & Wagoner 1993).

In § 2 we state our assumptions, introduce the differential equation that describes the normal modes, explain the boundary conditions that we use, and describe our method of solution. In § 3 we present and discuss the solutions of the warp equation when only the gravitomagnetic torque is included, when only the radiation warping torque is included, and when both torques are included. In § 4 we summarize our conclusions and discuss briefly the implications of our results for the observability of Lense-Thirring precession in X-ray binaries.

2. ASSUMPTIONS AND METHOD

In the work reported here we make several approximations to simplify the calculations and facilitate comparison with previous work. We have explored the normal modes of disks in the $1/r$ Newtonian gravitational potential and in several pseudopotentials. We treat the disk flow in the Newtonian approximation and include gravitomagnetic effects only to lowest post-Newtonian order. Therefore our treatment is accurate only outside the radius of the innermost stable circular orbit. We use an α model of the accretion

disk, setting $T_{r\phi} = \alpha P$ with α constant, and assume that the gas in the disk is fully ionized hydrogen.

In considering the radiation-warping torque we follow Pringle (1996), treating the central object as an isotropically radiating point source, treating the disk as a perfect absorber, and neglecting shadowing of the disk at larger radii by the disk at smaller radii. We also neglect the radial and drag forces caused by interaction of radiation from the central source with the gas orbiting in the disk and the torques produced by radiation of the kinetic energy dissipated within the disk (see Miller & Lamb 1996).

Following Petterson (1977a), we assume that the tilt of any given ring of gas is small and treat the accretion disk as a one-parameter family of rings that exchange angular momentum via advection and viscous torques. Writing the angular momentum per unit radial distance and azimuthal angle as $\Sigma R^3 \Omega \mathbf{l}$, where Σ is the local surface density of the disk, R is the radius, Ω is the angular velocity of the disk flow, and $\mathbf{l}(R)$ is the unit vector normal to the plane of the ring at R , the equation that expresses conservation of angular momentum is (compare Papaloizou & Pringle 1983, eq. [2.4])

$$\begin{aligned} \frac{\partial}{\partial t} (\Sigma R^3 \Omega \mathbf{l}) + \frac{\partial}{\partial R} (v_R \Sigma R^3 \Omega \mathbf{l}) \\ = \frac{\partial}{\partial R} \left[\Sigma R^3 \left(\nu_1 \frac{\partial \Omega}{\partial R} \mathbf{l} + \frac{1}{2} \nu_2 \Omega \frac{\partial \mathbf{l}}{\partial R} \right) \right] \\ + \frac{2G}{R^3 c^2} \mathbf{J} \times \mathbf{l} (\Sigma R^3 \Omega) - s \frac{RL}{12\pi c} \dot{\mathbf{z}} \times \frac{\partial \mathbf{l}}{\partial R}, \quad (1) \end{aligned}$$

where ν_1 is the R - ϕ viscosity, ν_2 is the R - z viscosity, L is the luminosity of the central source, and $\dot{\mathbf{z}}$ and \mathbf{J} are the spin axis and angular momentum of the star. The first term on the right side of equation (1) is the viscous torque, the term proportional to $\mathbf{J} \times \mathbf{l}$ is the gravitomagnetic torque produced by the spin of the compact object, and the term proportional to L is the radiation torque. The factor s in this term allows us to track the effect of the radiation torque: to include this torque we set $s = 1$; to neglect it, we set $s = 0$.

In this report we are most interested in gravitomagnetic precession of the disks around the neutron stars in the atoll and Z sources. These neutron stars are likely to have been spun up to their equilibrium spin rates (Lamb et al. 1985; Miller, Lamb, & Psaltis 1998; Psaltis et al. 1998). The z -component of the net flux of angular momentum through the disk, \dot{J}_z , is therefore zero. We therefore assume that the z -component of the net flux (which is equal to the component of

the net flux parallel to the axis of the disk, to first order in the tilt) is zero.

In order to simplify the presentation, the equations in the remainder of this section assume that the angular velocity in the disk is Keplerian in the $1/r$ Newtonian potential. (The generalization to pseudopotentials is straightforward.)

For Keplerian disks with zero net angular momentum flux along the z -axis, $v_R = (\nu_1/\Omega)(\partial\Omega/\partial R) = -(3/2)(\nu_1/R)$ everywhere. To facilitate comparison with previous work, we consider disks with power-law radial temperature profiles $T(R) = T_i(R/R_i)^{-\mu}$, where the subscript i indicates the value of the quantity at the inner radius of the calculation. In the α -disk model, $-\rho\nu_1 R(\partial\Omega/\partial R) = 2\alpha\rho k_B T/m_p$ and hence

$$\nu_1 = \frac{4\alpha k_B T_i}{3m_p(GM)^{1/2}} R_i^\mu R^{3/2-\mu}. \quad (2)$$

For simplicity, in the present work we take the ratio $\kappa \equiv \nu_2/\nu_1$ of the two kinematic viscosities to be independent of radius.

For small tilt angles, $\mathbf{l} \approx (\beta \cos \gamma, \beta \sin \gamma, 1)$ and hence the disk warp is completely specified locally by the tilt β and twist γ . Following Hatchett et al. (1981), we represent the warp by the real and imaginary parts of the complex variable $W \equiv \beta \cos \gamma + i\beta \sin \gamma = \beta e^{i\gamma}$. Then the component of equation (1) perpendicular to $\hat{\mathbf{z}}$ can be written as (compare Papaloizou & Pringle 1983, eq. [2.6])

$$\begin{aligned} \frac{\partial W}{\partial t} &= \frac{1}{2\Sigma R^3 \Omega} \frac{\partial}{\partial R} \left(\nu_2 \Sigma R^3 \Omega \frac{\partial W}{\partial R} \right) \\ &\quad + i \frac{2GJ}{R^3 c^2} W - is\Gamma \frac{\partial W}{\partial R}. \end{aligned} \quad (3)$$

Here

$$\Gamma \equiv L(12\pi\Sigma R^2\Omega c)^{-1} = G_0 R_i^\mu R^{1-\mu}, \quad (4)$$

where

$$\begin{aligned} G_0 &\equiv \frac{\epsilon\alpha k_B T_i}{3GMm_p} \\ &= 3.1 \times 10^{-4} \frac{\text{rad}}{\text{s}} \left(\frac{\epsilon}{0.2} \right) \left(\frac{\alpha}{0.05} \right) \left(\frac{T_i}{10^7 \text{K}} \right) \left(\frac{2M_\odot}{M} \right) \end{aligned} \quad (5)$$

is the characteristic angular frequency associated with the radiation torque at the inner edge of the disk, expressed in terms of the accretion efficiency ϵ . In writing the last expression on the right in equation (4),

we have used the mass continuity equation and the expression for the radial velocity.

We now change to the new radial variable

$$x \equiv (\epsilon/\kappa) (R/R_g)^{1/2}, \quad (6)$$

where $R_g \equiv GM/c^2$, and look for global modes of the disk of the form $W(t, R) = e^{i\eta t} W(x)$. Equation (3) then becomes

$$xW'' + (2 - isx)W' - i\left(A - \frac{B}{x^6}\right)\left(\frac{x}{x_i}\right)^{2\mu} W = 0, \quad (7)$$

where the prime denotes differentiation with respect to x ,

$$A \equiv 2\eta/G_0 \quad (8)$$

is the complex mode frequency scaled by G_0 , and

$$\begin{aligned} B &\equiv j \frac{4c}{G_0 R_g} \left(\frac{\epsilon}{\kappa} \right)^6 \\ &= \frac{1.7 \times 10^4}{\kappa^6} \left(\frac{j}{0.2} \right) \left(\frac{\epsilon}{0.2} \right)^5 \left(\frac{0.05}{\alpha} \right) \left(\frac{10^7 \text{K}}{T_i} \right) \end{aligned} \quad (9)$$

is the gravitomagnetic frequency at $x = 1$ scaled by G_0 , for a compact object with dimensionless angular momentum $j \equiv cJ/GM^2$.

The strong dependence of B on the accretion efficiency ϵ and viscosity ratio κ is an artifact of our choice $x \propto \epsilon/\kappa$ for fixed R . The gravitomagnetic precession frequency at a given radius R is independent of ϵ and κ , and the radius at which the gravitomagnetic and radiation torques are comparable therefore depends only weakly on ϵ and κ . Note also that if s is set to zero, so that the radiation torque is neglected, equation (7) becomes independent of ϵ , as it must; in this case ϵ is simply an arbitrary factor in the conversion from R to x and has no physical meaning.

Equation (7) is a linear, complex, second-order ordinary differential equation with complex frequency A . Specifying a solution of this equation, including the complex frequency, therefore requires six conditions. The tilt amplitude and twist angle at the inner edge of the disk are arbitrary, and hence only four conditions are physically meaningful. In general, the physics imposes two boundary conditions at the inner edge of the disk, at x_i , and two at the outer edge, at x_o . These boundary conditions restrict solutions to a countable set of “normal modes” $\beta(x)$ and $\gamma(x)$ corresponding to a discrete spectrum of precession frequencies $\omega = \text{Re } A$ and growth rates $\sigma = -\text{Im } A$.

Consider first the boundary conditions at the inner edge of the disk. The solution depends only on the ratio $W'(x_i)/W(x_i)$, because $W(x_i)$ is arbitrary. We have explored ratios from zero to extremely high values. In particular, we have considered $W'(x_i) = 0$, which corresponds to no external torque acting on the inner edge of the disk. We have also considered a variety of external torques that vary in time as $e^{i\eta t}$ and act on the inner edge of the disk, including a torque that forces $W(x_i) = 0$. This boundary condition corresponds to pinning of the inner edge of the disk in the rotation equator of the compact object and is only possible if there is a strong external torque.

Consider now the boundary conditions at the outer edge of the disk. If there is no torque on the outer edge of the disk, then $W'(x_o) = 0$. If instead the outer edge of the disk is pinned to the equatorial plane, for example by the accretion stream, the appropriate boundary condition would be $W(x_o) = 0$. For a detailed discussion of outer boundary conditions, see Maloney, Begelman, & Nowak (1998).

The warp equation (7) is very stiff when the gravitomagnetic torque is included. We therefore used the method of Kaps and Rentrop (see Press et al. 1992, § 16.6) to integrate the warp equation outward or inward, depending on the type of solution being sought (see § 3). In either case, we varied the precession frequency and the growth rate, iterating until the boundary condition at the other edge of the disk from which we started was satisfied. We have obtained approximate analytical solutions of the warp equation in a variety of asymptotic regimes, using the WKB method. These solutions will be reported in detail elsewhere (Marković & Lamb, in preparation). In many cases we used *locally* valid analytic solutions to start or guide the numerical integration. In some cases (see below) we were only able to find global numerical solutions after we had obtained locally valid analytic solutions of the same type. We have checked our global numerical solutions against our analytical solutions wherever possible.

3. RESULTS AND DISCUSSION

We have solved the warp equation (7) for the normal modes of the disk up to very high mode numbers for a variety of gravitational potentials, wide ranges of the relevant parameters, the different inner and outer boundary conditions discussed in the previous section, and a range of outer disk radii. In this first

report, we focus on our results for the undriven (free) modes of isothermal disks in the $1/r$ Newtonian gravitational potential, mentioning only in passing our results for modes driven at the inner edge of the disk and pseudopotentials that mimic the steeper effective potentials of general relativity.

We are particularly interested in gravitomagnetic precession of the disks around the neutron stars in the atoll and Z sources. As noted in § 2, these neutron stars are likely to have been spun up to their equilibrium spin rates, in which case \dot{J}_z , the z -component of the net flux of angular momentum through the disk, is zero. Therefore all the results reported here are for $\dot{J}_z = 0$. This assumption is not as restrictive as it might seem, because the tilt functions, precession frequencies, and damping rates of the disk warping modes are almost unaffected by the value of \dot{J}_z , unless it is almost equal to the flux being advected through the disk.

When only the gravitomagnetic torque is included, we have found two families of solutions: a set of low-frequency gravitomagnetic (LFGM) modes, all of which have frequencies less than a certain critical frequency ω_{crit} , and a set of high-frequency gravitomagnetic (HFGM) modes, all of which have frequencies greater than ω_{crit} . Using approximate analytical expressions valid for the high-order modes of an isothermal disk, we find (see Marković & Lamb, in preparation)

$$\omega_{\text{crit}} \approx (x_i/x_o)^{1/2} B / (11x_i^6), \quad (10)$$

where x_i and x_o are the dimensionless radii (see eq. [6]) of the inner and outer edges of the disk and B is given by equation (9).

The critical frequency can be understood qualitatively as follows. The precession frequency of a gravitomagnetic mode is a weighted average of the single-particle precession frequency over the radial extent of the mode, and hence ω_{crit} is roughly determined by the radius at which the mode function peaks. The tilt functions of the highest-order LFGM and HFGM modes all peak at about the same place in the disk, so their frequencies are almost identical. The value of x at which these modes peak scales with the dimensions of the disk as $x_i^{11/12} x_o^{1/12}$.

When only the radiation warping torque is included, we have found a family of low-frequency radiation-warping (R) modes. Our results for the tilt functions and precession frequencies of the low-order R modes agree well with previous results (Mal-

oney et al. 1996). When both the gravitomagnetic and radiation-warping torques are included, we have found a family of low-frequency gravitomagnetic radiation-warping (LFGMR) modes. The lowest-order LFGMR modes are essentially R modes, whereas the high-order LFGMR modes are essentially LFGM modes. In between there are a few hybrid modes that are affected by both the radiation-warping torque and the gravitomagnetic torque. The HFGM modes are essentially unaffected by any radiation warping torque.

All the results reported here are for $\kappa = 1$, $G_0 = 3.1 \times 10^{-4} \text{ rad s}^{-1}$, $B = 1.7 \times 10^4$, $x_i = 0.49$, and $x_o = 50$. This value of x_i corresponds to $R_i = 6 \text{ GM}/c^2$ for $\epsilon = 0.2$. If the outer radius of the disk is two or three times larger than assumed here, there would be a few additional modes with very low frequencies. The results shown for the R and HFGM modes assume $W'(x_i) = 0$ and $W'(x_o) = 0$; the results shown for the LFGM and LFGMR modes assume only $W'(x_o) = 0$.

Although in some cases the detailed shapes of the warp functions and the precise values of the frequencies and growth rates of the disk warping modes depend on the choice of parameters and boundary conditions, the general behavior of the modes is very similar to the results we present here. A detailed survey of parameters, boundary conditions, and gravitational potentials will be presented elsewhere (Marković & Lamb, in preparation).

3.1. Low-Frequency Gravitomagnetic Modes

The properties of the LFGM modes are determined primarily by the gravitomagnetic and viscous torques. These modes can therefore be found by integrating the warp equation (7) outward from the inner edge of the disk, using the analytical solution that is valid at small radii when the gravitomagnetic torque is dominant to start the integration. (If instead the warp equation is integrated inward, generally only solutions with unphysically large torques at the inner boundary can be found.)

The LFGM warp functions, precession frequencies, and damping rates are almost completely independent of the inner boundary condition. In particular, the LFGM modes do not depend on whether the disk is being driven at the inner boundary. The reason is that the gravitomagnetic and viscous torques cause the tilt function to converge to a characteristic shape that depends only on the mode number within a radial

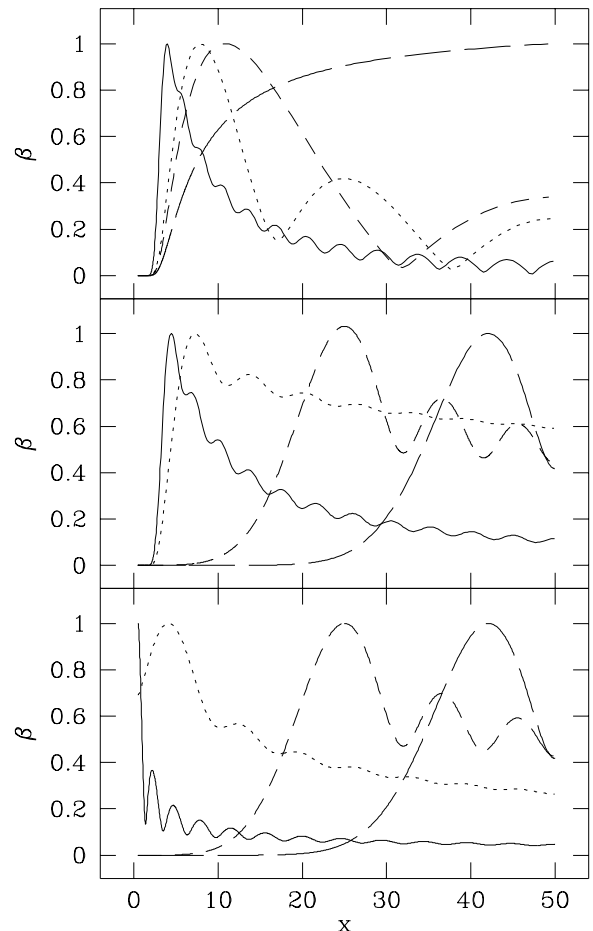


Fig. 1.— Tilt functions $\beta(x)$ for selected warping modes of the accretion disk, normalized to maximum values of unity. *Top*: Low-frequency gravitomagnetic (LFGM) modes. Shown are the static $n = 0$ mode (long dashes) and the time-dependent $n = 1$ (short dashes), $n = 2$ (dots), and $n = 12$ (solid line) modes. *Middle*: Low-frequency gravitomagnetic radiation-warping (LFGMR) modes. Shown are the time-dependent $n = 1$ (long dashes), $n = 3$ (short dashes), $n = 7a$ (dots), and $n = 12$ (solid line) modes. *Bottom*: Radiation-warping (R) modes. Shown are the time-dependent $n = 1$ (long dashes), $n = 3$ (short dashes), $n = 7$ (dots), and $n = 12$ (solid line) modes.

distance from the inner edge that is extremely small compared to the radial extent of the mode, regardless of what is happening at the inner boundary. The properties of the low-order precessing LFGM modes

depend only weakly on which boundary condition is imposed at x_0 and the value of x_0 , because even these modes are large only near the inner edge of the disk. The properties of the higher-order LFGM modes are essentially independent of the outer boundary condition and the radius of the outer boundary. All LFGM modes are independent of the accretion efficiency ϵ .

The tilt functions $\beta(x)$ of four selected LFGM modes are shown in the top panel of Figure 1. We define the LFGM “mode number” n loosely as the number of peaks in $\beta(x)$. The fundamental ($n = 0$) LFGM mode is static ($\omega = \sigma = 0$). This mode reflects the tendency of the gravitomagnetic and viscous torques to align the axis of the inner disk with the spin axis of the compact object (Bardeen & Petterson 1975). Strictly speaking, for the $n = 0$ mode W' approaches zero at large x only asymptotically; however, W' is already very close to zero at $x = 50$. All the time-dependent LFGM modes (those with $n > 0$) precess in the prograde direction ($\omega > 0$) and are damped ($\sigma < 0$).

Figure 2 shows the growth rates and precession frequencies of the lowest ~ 20 LFGM modes. As n increases, the relative spacing $\Delta\omega/\omega$ between adjacent modes decreases and the spectrum therefore becomes quasi-continuous at large n . The spectrum of the precession frequencies and damping rates of the higher-order LFGM modes is plotted as a continuous curve in Figure 3. The slight break in the spectrum at $\omega \sim 10^2$ is where the damping rate becomes comparable to ω_{crit} .

The very high-order LFGM modes are spiral corrugations of the inner disk that have very short wavelengths and extend from the radius r_i of the inner edge of the disk to $\sim 10r_i$. Their tilt functions have a single smooth peak, but the phase of the warp changes by a very large amount in a very short radial distance. When the radial distance between corrugations becomes comparable to or shorter than the vertical thickness of the disk, treating the disk thickness as infinitesimal is no longer valid. The dotted portion of the LFGM spectrum shown in Figure 3 shows where this distance becomes smaller than $10^{-2}r$. At this point the precession frequency ω is 2×10^3 , which corresponds to a circular frequency $f \equiv \text{Re } \eta / 2\pi = \omega G_0 / 4\pi \approx 0.05$ Hz.

The precession frequencies of the LFGM modes increase with n , but only up to $\omega_{\text{crit}} \sim 1.2 \times 10^4$ for $\epsilon = 0.2$ and $x_i = 0.49$. As n increases further, ω remains $\sim 1.2 \times 10^4$, which corresponds to a circular

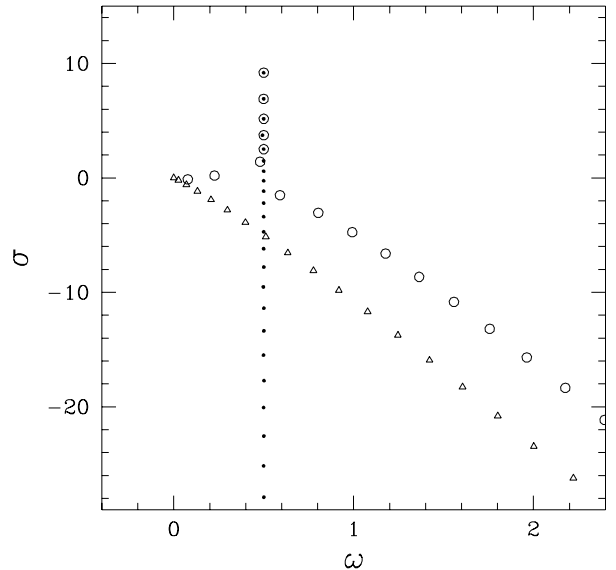


Fig. 2.— Spectrum of growth rates σ and precession frequencies ω of the lowest ~ 20 low-frequency gravitomagnetic (LFGM) modes (open triangles), radiation-warping (R) modes (dots), and low-frequency gravitomagnetic radiation-warping (LFGMR) modes (open circles) of the accretion disk.

frequency ~ 1 Hz for a compact object of solar mass. The reason is that as n increases, the LFGM modes at first become more localized near the inner edge of the disk but eventually stop becoming localized. Hence, the precession frequency stops rising. This is the case not only for the free LFGM modes but also for LFGM modes driven at the inner boundary and for the LFGM modes in pseudopotentials that mimic the effective potential of general relativity. Thus, *all LFGM modes have precession frequencies $\lesssim 1$ Hz for compact objects of solar mass.*

The damping rates of even the lowest-order precessing LFGM modes are $\gtrsim 10$ times higher than their precession frequencies. For example, the precession frequencies and growth rates of the LFGM modes shown in Figure 1 are $\omega = 0.026$, $\sigma = -0.209$ for $n = 1$; $\omega = 0.071$, $\sigma = -0.599$ for $n = 2$; and $\omega = 1.25$, $\sigma = -13.7$ for $n = 12$. As n increases, the damping rate increases faster than the precession frequency (see Fig. 2). Thus, modes with precession frequencies $\omega \approx 100$ have damping ratios $|\sigma|/\omega \gtrsim 20$. At the critical frequency ($\omega_{\text{crit}} \sim 1.2 \times 10^4$), the damping ratio exceeds 1.5×10^3 . Hence, *all precessing LFGM modes are highly overdamped.*

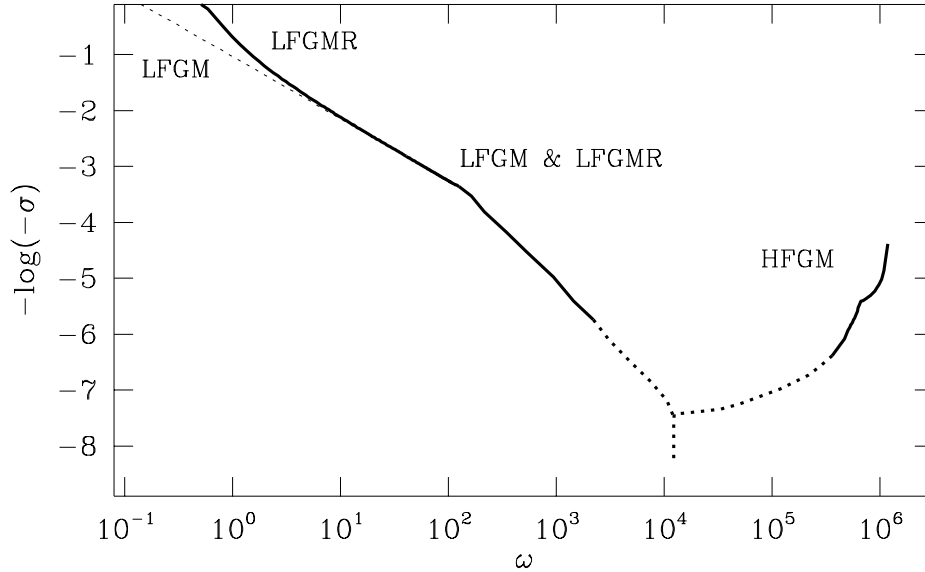


Fig. 3.— Spectrum of damping rates $-\sigma$ and precession frequencies ω of low-frequency gravitomagnetic (LFGM) modes (dotted line), low-frequency gravitomagnetic radiation-warping (LFGMR) modes (left solid line), and high-frequency gravitomagnetic (HFGM) modes (right solid line) plotted as continuous curves. The damping rates of the LFGM and LFGMR modes with ω greater than ~ 10 are indistinguishable on this scale. The LFGM and HFGM spectra become almost vertical at the critical frequency ω_{crit} discussed in the text. The HFGM spectrum is essentially unaffected by any radiation warping torque. The dotted portions of the curves show where the radial distance between corrugations becomes smaller than $10^{-2} r$.

3.2. Radiation Warping Modes

It has been suggested (e.g., Stella 1997a, 1997b) that the radiation warping torque discussed by Pringle (1996) and Maloney et al. (1996) may drive gravitomagnetic precession modes of the inner disk. We have investigated the effects of this torque on the precession frequencies and damping rates of gravitomagnetic modes.

We first discuss the normal modes of the disk when the radiation-warping torque is included but the gravitomagnetic torque is not. These modes can be readily found by numerically integrating the warp equation (7) outward from the inner boundary or inward from the outer boundary, because the warp equation is not stiff when the gravitomagnetic torque is neglected.

The detailed shapes of the low-order R-mode tilt functions are affected by which boundary condition is imposed at the outer edge of the disk at x_o and by the value of x_o . In contrast, the tilt functions of the high-order R modes are strongly concentrated near the inner edge of the disk and hence are almost

unaffected by which boundary condition is imposed at x_o or the value of x_o . The high-order R-mode tilt functions typically become steep very near the inner boundary at x_i , even though $\beta'(x_i) = 0$, because $\beta''(x_i)$ is large.

Although the tilt functions of the high-order R modes are almost unaffected by which boundary condition is imposed at x_o or the value of x_o , the precession frequencies of *all* the R modes depend on which boundary condition is imposed at the outer boundary.

The tilt functions $\beta(x)$ of four R modes are shown in the bottom panel of Figure 1. We find that the tilt functions of the lowest-order R modes are appreciable only at large radii, in agreement with previous work (Maloney et al. 1996). The precession frequencies of the half-dozen lowest-order R modes are therefore independent of the inner boundary condition.

The dots in Figure 2 show the growth rates and precession frequencies of the lowest ~ 20 R modes. We find that all R modes that satisfy $W'(x_i) = W'(x_o) = 0$ precess in the prograde direction with frequency $\omega = 0.5$. The growth rates of the four low-order R modes

shown in Figure 1 are $\sigma = 9.19$ for $n = 1$, which is the lowest-order R mode; $\sigma = 5.16$ for $n = 3$; $\sigma = 0.58$ for $n = 7$; and $\sigma = -4.72$ for $n = 12$. The growth rate falls steeply with increasing mode number, and modes with $n \gtrsim 10$ are very strongly damped. For fixed mode number n , the growth rate increases with increasing x_o , i.e., $d\sigma/dx_o > 0$.

We also find that all the R modes that satisfy $W(x_i) = W(x_o) = 0$ precess in the prograde direction with frequency $\omega = 1$. This is the same precession frequency found by Maloney et al. (1996) for all the R modes that satisfy $x^2 W'(x) \rightarrow 0$ as $x \rightarrow 0$ instead of $W'(x_i) = 0$. This degeneracy of R-mode precession frequencies is peculiar to isothermal disks: for more general temperature profiles, different R modes precess at different rates (see Maloney et al. 1998). On the other hand, for R modes that satisfy “mixed” boundary conditions, either $W(x_i) = W'(x_o) = 0$ or $W'(x_i) = W(x_o) = 0$, the higher-order modes precess at slightly different frequencies from the lowest-order modes. For $W(x_i) = W'(x_o) = 0$, most modes precess in the prograde direction, but the torque acting on the inner edge of the disk causes the tilt function of one of the low-order modes to increase monotonically with increasing x , i.e., $\beta'(x)$ is positive everywhere. This mode precesses very slowly, either in the prograde or the retrograde sense, depending on the value of x_o , and is either weakly growing or weakly damped (see Marković & Lamb, in preparation).

3.3. Low-Frequency Gravitomagnetic Radiation Warping Modes

Consider now the low-frequency normal modes of the disk when both the gravitomagnetic torque and the radiation warping torque are included. These are the LFGMR modes. These modes can be found by integrating the warp equation (7) outward from the inner edge of the disk, using the same approach that was used to find the LFGM modes.

The character of the LFGMR modes changes with increasing mode number. Like the tilt functions of the low-order R modes, the tilt functions of the low-order LFGMR modes are appreciable only at large radii and are affected by which boundary condition is imposed at x_o and by the value of x_o . Like the precession frequencies of all the R modes, the precession frequencies of the low-order LFGMR modes depend on which boundary condition is imposed at the outer boundary, but not on the value of x_o . Unlike the R modes but like the LFGM modes, the frequencies and damping

rates of the LFGMR modes are almost completely independent of the inner boundary condition, for the same reason that this is true of the LFGM modes. The properties of the high-order LFGMR modes are only weakly dependent on the boundary condition at x_o and the value of x_o . Only the properties of the lowest-order LFGMR modes depend on the accretion efficiency ϵ .

For the parameter values considered in this report, the first six LFGMR modes are appreciable only at large radii and hence are virtually unaffected by the gravitomagnetic torque. Their tilt functions, precession frequencies, and growth rates are essentially identical to those of the first six R modes (see Figs. 1 and 2), except that the very innermost part of the disk is forced into the rotation equator of the central object by the combined action of the gravitomagnetic and internal viscous torques, as first discussed by Bardeen & Petterson (1975). This is the reason that the properties of the lowest-order LFGMR modes do not depend on the boundary condition at the inner edge of the disk.

Like the low-order radiation warping modes, the lowest-order LFGMR modes precess in the prograde direction with precession frequencies of either 0.5 or 1.0, depending on whether the inner and outer edges of the disk are free or pinned in the disk plane. For a compact object of solar mass, these precession frequencies are $\sim 10^{-5}$ Hz. Also like the low-order radiation warping modes, the lowest-order LFGMR modes are all growing modes.

There are typically two or three LFGMR modes that are hybrid gravitomagnetic radiation-warping modes. The shapes of these modes are very similar to the radiation-warping modes in the outer disk, except that the combined action of the gravitomagnetic and internal viscous torques again forces the very innermost part of the disk into the rotation equator of the central object. The hybrid gravitomagnetic radiation-warping modes generally (but not always; see below) precess in the prograde direction with precession frequencies between $\sim 10^{-6}$ Hz, for a compact object of solar mass (~ 0.08 in our dimensionless units), and the $\sim 10^{-5}$ Hz frequency of the radiation-warping modes. These modes are either weakly damped or weakly growing. Thus, when the radiation-warping torque is taken into account, there is generally no time-independent mode: the Bardeen-Petterson mode becomes weakly time-dependent.

For some values of x_o there is a single mode that

precesses slowly in the *retrograde* direction and is either weakly growing or weakly damped. For this mode, the gravitomagnetic torque plays a role analogous to that of the inner boundary torque for R modes with $W(x_i) = W'(x_o) = 0$, pinning the disk to the rotation equator of the central object. For a special choice of the parameters B and x_o , there is a single static mode ($\omega = \sigma = 0$). However, because of the fine tuning required, this situation is unlikely to be of any practical importance.

The tilt functions of four low-order LFGMR modes are shown in the middle panel of Figure 1. The frequencies and growth rates of these modes are $\omega = 0.5$, $\sigma = 9.19$ for $n = 1$, which is the lowest-order LFGMR mode; $\omega = 0.5$, $\sigma = 5.16$ for $n = 3$; $\omega = 0.23$, $\sigma = 0.20$ for $n = 7a$ (see below); and $\omega = 1.18$, $\sigma = -6.62$ for $n = 12$. The growth rates and precession frequencies of the lowest ~ 20 LFGMR modes are shown in Figure 2.

For the parameter values used in the present study, there are two LFGMR modes that have tilt functions with 7 peaks. The tilt function, precession frequency, and growth rate of the $n = 7a$ LFGMR mode shown in Figure 1 are intermediate between those of the $n = 7$ R mode and the static LFGM mode. This is a growing mode that precesses in the prograde direction with a very low frequency and grows only very slowly (see Fig. 2). There is also another LFGMR mode with seven peaks, which we denote 7b; it precesses in the prograde direction with an even lower frequency ($\omega = 0.08$; again see Fig. 2) and is very weakly damped ($\sigma = -0.12$). This LFGMR mode is the static gravitomagnetic mode, weakly perturbed by the radiation torque.

All LFGMR modes with $n > 7$ are damped, but less so than LFGM modes with about the same frequency. These LFGMR modes are only weakly affected by the boundary condition at x_o or the value of x_o . The properties of the high-order LFGMR modes are almost identical to those of the LFGM modes with the same frequency. In particular, *all but the lowest-order LFGMR modes are highly over-damped* (the damping ratios of modes with $\omega \gtrsim 5$ are $\gtrsim 10$). Also, with increasing mode number, ω asymptotically approaches $\sim 1.2 \times 10^4$ for a disk inner edge at $x_i = 0.49$ (see Fig. 3). Again, this result holds even if the disk is driven at its inner edge and even for potentials that are steeper than the $1/r$ Newtonian potential. Thus, *all LFGMR modes have precession frequencies $\lesssim 1$ Hz for compact objects of solar mass.*

3.4. High-Frequency Gravitomagnetic Modes

The properties of the HFGM modes, which are all confined very near the inner edge of the disk, are determined primarily by the gravitomagnetic torque. If the warp equation is integrated outward, generally only the LFGM modes can be found, as noted in § 3.1. Although the HFGM modes can in principle be found by integrating the warp equation (7) inward from the outer edge of the disk, this is generally impractical. The reason is threefold. First, the warp functions of the HFGM modes increase by a factor of up to $\sim 10^{7,000}$ in going from the outer edge of the disk to their peak values, which occur very near the inner edge. Second, solving for the mode functions requires searching the two-dimensional ω - σ space for the precise complex frequencies that give valid solutions of the warp equation with the boundary conditions chosen. The signature of a valid solution is a mode function that is well-behaved at the inner edge of the disk, but because even valid solutions grow very large as the integration proceeds, valid and invalid solutions are not easily distinguishable without integrating the warp equation all the way to the inner edge of the disk, which is computationally inefficient. Third, the warp equation is very stiff at the high frequencies of these modes, so searching numerically for the complex frequencies of the valid solutions is difficult.

The lowest-order (highest-frequency) HFGM modes were initially found by using analytical solutions valid for large ω to start the inward numerical integration at $x \approx 0.6$, i.e., at an x value $\sim 20\%$ larger than the x value at the inner edge of the disk. Starting at this x value, the HFGM mode functions typically increase by only a factor of 10^{50} – 10^{100} between the starting point and their peak, so the search for solutions in the ω - σ plane is much more efficient. Of course, once the complex frequency of a solution is accurately known, the warp equation can be integrated all the way from the outer edge of the disk to its inner edge. Moreover, once one valid solution has been found, additional solutions can be found relatively easily.

Unlike the LFGM and LFGMR modes, the warp functions, precession frequencies, and damping rates of the HFGM modes are affected by the boundary condition at the inner edge of the disk. In particular, the properties of the HFGM modes depend on whether the disk is being driven at its inner boundary. A strong driving torque at the inner edge of the disk can excite a variety of HFGM modes, depending

on its time dependence and components parallel and perpendicular to the angular momentum of the gas in the disk. A driving torque that oscillates with any given frequency can excite a driven HFGM mode with that same frequency, if the torque is strong enough.

The frequencies and damping rates of the HFGM modes are only slightly affected if the Newtonian gravitational potential is replaced by a pseudopotential that mimics the steeper effective potentials of general relativity. The HFGM modes are almost independent of the outer boundary condition and the radius of the outer boundary. They are essentially unaffected by the radiation warping torque and hence do not depend on the accretion efficiency ϵ .

Here we focus on the undriven (free) HFGM modes, which are the relevant HFGM modes when there is no torque acting on either the inner or the outer edge of the disk. These HFGM modes satisfy $W'(x_i) = 0$ and $W'(x_o) = 0$. All the free HFGM modes are time-dependent, precess in the prograde direction ($\omega > 0$), and are damped ($\sigma < 0$).

We define the HFGM mode number m by counting downward in frequency, starting with $m = 1$. The tilt functions $\beta(x)$ of four low-order free HFGM modes are shown in Figure 4. All have a single very narrow peak near the inner edge of the disk. These modes are very localized, tightly wound spiral corrugations of the disk very near its inner edge. The radial distance between the corrugations of the lowest dozen or so HFGM modes decreases with increasing mode number, although not smoothly, whereas the overall radial width of the tilt function increases with increasing mode number, approximately linearly for $m > 2$ up to $m \sim 14$.

Even though the HFGM warp functions are tightly wound, the two lowest-order HFGM modes have relatively small winding numbers $N \equiv |\Delta\gamma|/2\pi$, where $\Delta\gamma$ is the change in phase over the radial interval where the mode has appreciable amplitude: N is ~ 0.5 for $m = 1$ and ~ 1 for $m = 2$. Hence these two modes disturb significantly the azimuthal symmetry of the disk. In contrast, the high-order HFGM modes have high winding numbers and are therefore almost axisymmetric. This is illustrated in Figure 5, which shows the real and imaginary parts of the warp functions for the $m = 1$, $m = 2$, and $m = 8$ HFGM modes.

The lowest-order free HFGM modes precess with frequencies comparable to the gravitomagnetic pre-

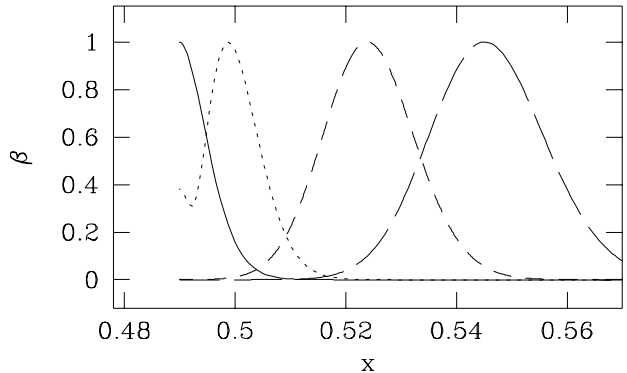


Fig. 4.— Tilt functions $\beta(x)$ of four low-order undriven high-frequency gravitomagnetic (HFGM) modes, normalized to maximum values of unity. Shown are the time-dependent $m = 1$ (solid line), $m = 2$ (dots), $m = 8$ (short dashes) and $m = 14$ (long dashes) modes.

cession frequency $\omega_{\text{gm},i} = B/x_i^6$ of a particle at the inner edge of the disk. The highest possible precession frequency is therefore the gravitomagnetic precession frequency at the innermost stable circular orbit. The lowest-order free HFGM modes are weakly damped.

Specifically, the precession frequencies and growth rates of the first few HFGM modes are $\omega = 1.19 \times 10^6 = 0.97\omega_{\text{gm},i}$, $\sigma = -2.40 \times 10^4$ for $m = 1$; $\omega = 1.10 \times 10^6$, $\sigma = -7.32 \times 10^4$ for $m = 2$; $\omega = 1.04 \times 10^6$, $\sigma = -1.05 \times 10^5$ for $m = 3$; $\omega = 8.22 \times 10^5$, $\sigma = -2.02 \times 10^5$ for $m = 8$; and $\omega = 6.53 \times 10^5 = 0.53\omega_{\text{gm},i}$, $\sigma = -2.87 \times 10^5$ for $m = 14$. The Q ($\equiv -\omega/\sigma$) values of these modes range from 49 for the $m = 1$ mode to 2.3 for the $m = 14$ mode. The damping rates of these modes increase with increasing viscosity. For example, if the viscosity parameter α (see § 2) is 0.5 rather than 0.05, the Q of the fundamental HFGM mode becomes 22 rather than 49.

Figure 6 shows the individual growth rates and precession frequencies of the eleven lowest-order (highest-frequency) free HFGM modes; the growth rates and precession frequencies of the next higher-order HFGM modes are indicated by the dotted curve. The frequencies of the HFGM modes at first decrease steadily with increasing mode number, but the separation between adjacent modes in the ω, σ plane shrinks rapidly with further increases in the mode number and the spectrum becomes quasi-continuous.

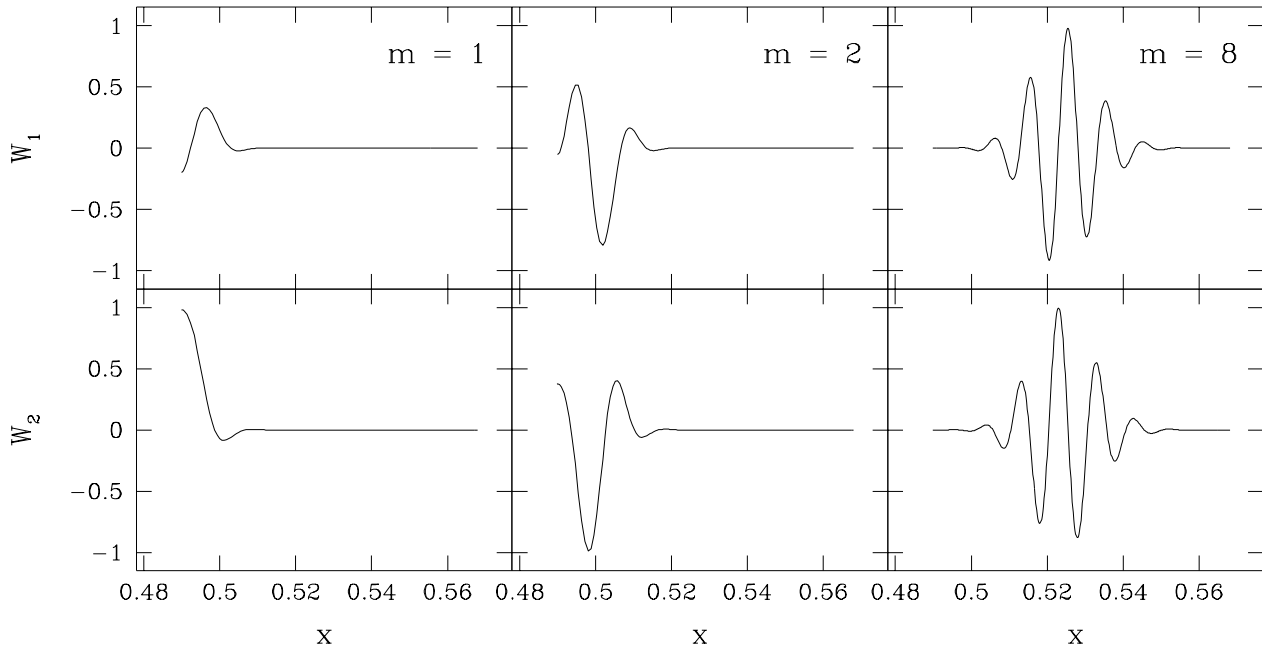


Fig. 5.— Real and imaginary parts $W_1(x)$ and $W_2(x)$ of the tilt function W for the $m = 1$, $m = 2$, and $m = 8$ HFGM modes. The tilt functions $\beta(x)$ of these three modes are shown in Figure 4.

The spectrum of damping rates and precession frequencies of the free HFGM modes up to very high order are plotted as a continuous curve in Figure 3, together with the spectrum of the free LFGM and LFGMR modes for comparison. The dotted portion of the HFGM spectrum shown in Figure 3 shows where the radial distance between corrugations becomes smaller than $10^{-2}r$. The corresponding precession frequency ω is 4×10^5 , which is 10 Hz.

As Figure 3 shows, the damping rate increases steadily with increasing mode number. At $m \sim 15$ ($\omega \approx 6.3 \times 10^5$), Q has fallen to about unity ($\sigma \approx -1.1 \times 10^6$). The ω - σ spectrum breaks at this frequency, because the damping rates of the higher-order modes increase even more rapidly with decreasing ω as the mode functions broaden and their winding numbers increase.

As the mode number increases further and the precession frequency approaches ω_{crit} from above, the spectrum turns sharply downward, because the damping rate continues to grow whereas the frequency approaches the constant critical frequency ω_{crit} from above. In the limit $\omega \rightarrow \omega_{\text{crit}}$, $\sigma \rightarrow -\infty$, the tilt functions of the HFGM modes assume the same shape $\beta_{\text{crit}}(x)$ (which peaks near $x = 1$) assumed by the

tilt functions of the LFGM modes as $\omega \rightarrow \omega_{\text{crit}}$ from below. Hence, *all the HFGM modes have precession frequencies between ~ 1 Hz and ~ 30 Hz for compact objects of solar mass.* Although the high-order free HFGM modes are very strongly damped, *the lowest-order HFGM modes are only weakly damped.*

4. SUMMARY AND CONCLUSIONS

We have found two families of disk warping modes in the presence of gravitomagnetic and radiation-warping torques. In general, all of these modes are time-dependent. In particular, the static mode found by Bardeen & Petterson (1975) is perturbed by the radiation-warping torque and becomes weakly time-dependent.

The low-frequency gravitomagnetic radiation-warping (LFGMR) modes have precession frequencies that range from the lowest frequency allowed by the size of the disk, which in dimensionless units (see § 2) is ~ 0.1 for the parameter values used in the present study, up to the critical frequency ω_{crit} (see eq. [10]), which is $\sim 1.2 \times 10^4$. The high-frequency gravitomagnetic (HFGM) modes have precession frequencies that range from ω_{crit} up to slightly less than the gravito-

magnetic precession frequency $\omega_{\text{gm},i}$ of a particle at the inner edge of the disk, which is $\sim 1.2 \times 10^6$ for the parameter values used in the numerical computations reported here. The HFGM modes are essentially unaffected by any radiation-warping torque.

The damping rates and frequencies of the modes in both families are changed by $\lesssim 10\%$ if the $1/r$ Newtonian potential is replaced by any of several pseudopotentials that mimic the steeper effective gravitational potentials of general relativity, because the properties of the modes at the inner edge of the disk are determined primarily by the gravitomagnetic torque.

The vast majority of the modes that lie between the lowest-frequency LFGMR modes and the highest-frequency HFGM modes are very short-wavelength corrugations of the disk and are very highly overdamped. In particular, the modes with frequencies in the interval $2 \times 10^3 < \omega < 4 \times 10^5$ have corrugation wavelengths $\lesssim 1\%$ of the radius at which the mode peaks. When the wavelength becomes less than the vertical thickness of the disk, our treatment of the disk as infinitesimal is no longer valid (see, e.g., Papaloizou & Pringle 1983). In this regime, modes of the type we have found may be even more strongly damped or even nonexistent.

4.1. The LFGMR Modes

The half-dozen lowest-order (lowest-frequency) LFGMR modes have essentially the same shapes as the previously known low-order radiation warping modes (Maloney et al. 1996), except that the very innermost part of the disk is forced into the rotation equator of the central object by the combined action of the gravitomagnetic and internal viscous torques, as first discussed by Bardeen & Petterson (1975). This is the reason that, unlike the radiation-warping modes, the low-order LFGMR modes do not depend on the boundary condition at the inner edge of the disk.

The lowest-order LFGMR modes precess in the prograde direction with precession frequencies of either 0.5 or 1.0 in dimensionless units, depending on whether the outer edge of the disk is free or pinned in the disk plane. This is the same precession behavior displayed by the low-order radiation warping modes. For a compact object of solar mass, these modes precess with frequencies $\sim 10^{-5}$ Hz. The lowest-order LFGMR modes, like the low-order radiation warping modes, are growing modes.

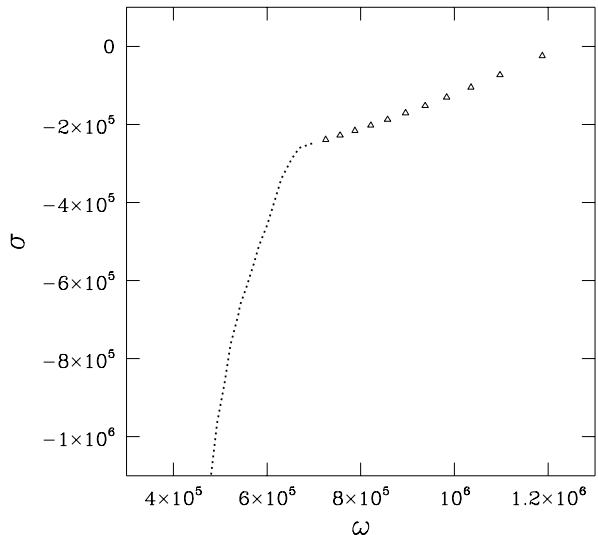


Fig. 6.— Spectrum of growth rates σ and precession frequencies ω of undriven high-frequency gravitomagnetic (HFGM) modes of the accretion disk. The frequencies and damping rates of the eleven lowest-order (highest-frequency) HFGM modes are plotted individually as open triangles. The dense spectrum formed by the precession frequencies and damping rates of the higher-order HFGM modes is indicated by the dotted line.

Typically two or three low-order LFGMR modes have properties intermediate between the gravitomagnetic modes and the radiation-warping modes. These hybrid modes are similar in shape to the radiation-warping modes of the same order, except that their tilt functions go to zero at the inner edge of the disk because of the combined action of the gravitomagnetic and internal viscous torques. The hybrid modes generally (but not always) precess in the prograde direction and are either weakly damped or weakly growing. For a compact object of solar mass, the precession frequencies of these modes lie between $\sim 10^{-6}$ Hz and $\sim 10^{-5}$ Hz, which is the frequency of the lowest-order LFGMR modes.

With increasing mode number, the frequencies of the LFGMR modes at first increase steadily but eventually approach ω_{crit} asymptotically from below. This happens even if the disk is driven at its inner edge. The LFGMR modes that have precession frequencies $\gtrsim 10^{-4}$ Hz are essentially unaffected by even a strong radiation-warping torque and have damping rates $\gtrsim 10$ times their frequencies. The highest-

frequency LFGMR modes are very short-wavelength spiral corrugations that extend from the radius r_i of the inner edge of the disk only to $\sim 10 r_i$. These modes have precession frequencies $\sim \omega_{\text{crit}}$, which is ~ 1 Hz for a compact object of solar mass, and are very strongly damped.

The hybrid gravitomagnetic radiation-warping modes that are excited by the radiation-warping torque may be of interest observationally, if they grow to significant amplitudes. These modes have very low frequencies, as much as an order of magnitude lower than the lowest-frequency modes known previously.

The high-frequency LFGMR modes appear unpromising as an explanation of the 6–300 Hz QPOs observed in some accreting neutron stars and black hole candidates, both because they are very strongly damped and because they have frequencies $\lesssim 1$ Hz for compact objects of solar mass. Excitation of high-frequency LFGMR modes by impulsive disturbances or a broad spectrum of fluctuations is unlikely to produce peaks in the brightness power spectrum with relative widths $\delta\nu/\nu$ as small as the ~ 0.5 –1 widths of the broad bumps observed in the frequency range ~ 20 –40 Hz in some atoll sources, let alone as small as the ~ 0.1 –0.3 widths of the QPO peaks observed in the Z sources and a several black-hole candidates. A narrow peak could be created by exciting these modes with a nearly monochromatic driving force, but then the QPO would not be generated by Lense-Thirring precession but by the driving force and would have a frequency and coherence unrelated to the properties of the gravitomagnetic modes of the inner disk. Moreover, the amplitudes of these modes would be limited by their very high damping rates.

4.2. The HFGM Modes

The tilt functions of the lowest-order (highest-frequency) undriven HFGM modes have a single very narrow peak near the inner edge of the disk. These modes are very localized spiral corrugations of the inner disk. The lowest-order undriven HFGM modes precess in the prograde direction with precession frequencies comparable to the gravitomagnetic precession frequency $\omega_{\text{gm},i} = B/x_i^6$ at the inner edge of the disk.

The damping rate of a mode is determined by the radial spacing δ between the disk corrugations. The damping rates $-\sigma$ of the highest-frequency undriven HFGM modes are given fairly accurately by

$-\sigma \approx \pi^2 x_{\text{max}}/\delta^2$, where x_{max} is the position of the maximum of the tilt function for the mode. Our numerical solutions show that for the dozen or so highest-frequency HFGM modes, δ decreases with increasing mode number, but not smoothly, whereas the radial width Δ of the tilt function increases approximately linearly with increasing mode number for $m > 2$ up to at least $m \sim 14$.

With increasing mode number, the frequencies of the HFGM modes at first decrease steadily. The dozen or so lowest-order HFGM modes have precession frequencies that range from $\approx \omega_{\text{gm},i}$ for the $m = 1$ mode to $\sim 0.5 \omega_{\text{gm},i}$ for the $m = 14$ mode. These modes are underdamped, with Q values that range from 49 for the $m = 1$ mode to 2.3 for the $m = 14$ mode. The damping rates of the HFGM modes are sensitive to the viscosity in the disk. If the viscosity parameter α (see § 2) is 0.5 rather than 0.05, for example, the Q of the fundamental HFGM mode becomes 22 rather than 49.

With further increases in the mode number, the HFGM modes become overdamped and their precession frequencies eventually approach ω_{crit} asymptotically from above. The highest-order HFGM modes are very short-wavelength spiral corrugations that extend from the radius r_i of the inner edge of the disk only to $\sim 10 r_i$. With increasing mode number, the shapes of the HFGM modes gradually approach the asymptotic shape of the highest-order LFGMR modes. Like the highest-order (highest-frequency) LFGMR modes, the highest-order (lowest-frequency) HFGM modes have precession frequencies $\sim \omega_{\text{crit}}$, which is ~ 1 Hz for a compact object of solar mass, and are very strongly damped.

The warp functions, precession frequencies, and damping rates of the modes in the HFGM family depend on the boundary condition at the inner edge of the disk. They are, for example, affected by whether there is a driving torque acting on the inner edge. Such a torque can excite a variety of HFGM modes, in addition to the free HFGM modes, depending on its time dependence and its components parallel and perpendicular to the angular momentum of the gas in the disk. A torque that oscillates with a given frequency and acts on the inner edge of the disk can always resonantly excite the appropriate driven HFGM mode that has the same frequency, if the torque is strong enough.

The properties of the HFGM modes are only slightly affected if the Newtonian gravitational potential is re-

placed by a pseudopotential that mimics the steeper effective potential at small radii in general relativity. The HFGM modes are also almost independent of the outer boundary condition and the radius of the outer boundary.

The high-frequency HFGM modes may be involved in some of the rapid X-ray variability and high-frequency QPOs observed in some accreting neutron stars and black hole candidates. The highest possible frequency of the fundamental (lowest-order, highest-frequency) HFGM mode is the gravitomagnetic precession frequency of gas at the radius R_{isco} of the innermost stable circular orbit around the compact object. For a compact object with mass M and dimensionless angular momentum $j \equiv cJ/GM^2 \ll 1$, $R_{\text{isco}} \approx 6GM/c^2$ and hence the Lense-Thirring precession frequency of the innermost stable circular orbit is

$$\nu_{\text{gm,isco}} \approx 30 \left(\frac{j}{0.2} \right) \left(\frac{2M_{\odot}}{M} \right) \text{ Hz} . \quad (11)$$

The largest value of j expected for neutron stars with spin frequencies ~ 300 Hz is ~ 0.2 . Hence, for a $2M_{\odot}$ neutron star with a radius smaller than that of the innermost stable circular orbit and a spin frequency ~ 300 Hz, the *highest possible* frequency of the fundamental HFGM mode would be ~ 30 Hz. The dozen lowest-order HFGM modes, which are weakly damped, would then have frequencies ranging from ~ 30 Hz down to ~ 10 Hz. For a $6M_{\odot}$ black hole with $j \sim 0.2$, the *highest possible* frequency of the fundamental HFGM mode would be ~ 10 Hz and the dozen lowest-order HFGM modes would have frequencies ranging from ~ 10 Hz down to ~ 5 Hz.

As mentioned in § 1, Stella & Vietri (1998) have recently suggested that gravitomagnetic precession of the inner disk may be responsible both for the broad bumps that are observed in the power spectra of some atoll sources between 20 and 40 Hz, and for the horizontal branch QPO, which is observed in the Z sources and appears as a strong, narrow peak that varies in frequency from 15 to 65 Hz. They proposed that these power spectral features are caused by gravitomagnetic precession of gas at the same radius as the gas in circular Keplerian orbit that is thought to generate the kilohertz QPOs (see Strohmayer et al. 1996; Miller et al. 1998), which have frequencies ranging from 900 to 1200 Hz in the sources they considered.

In the picture proposed by Stella & Vietri (1998), the gravitomagnetic precession frequency ν_{gm} , the fre-

quency ν_{K} of the Keplerian-frequency kilohertz QPO, and the dimensionless angular momentum j of the star are related by

$$\nu_{\text{gm}} = (GM4\pi/c^3) j \nu_{\text{K}}^2 . \quad (12)$$

Solving this relation for I_{45} , the moment of inertia of the star in units of 10^{45} g cm^2 , yields

$$I_{45} \left(\frac{M_{\odot}}{M} \right) = 2 \left(\frac{\nu_{\text{gm}}}{40 \text{ Hz}} \right) \left(\frac{300 \text{ Hz}}{\nu_{\text{K}}} \right) \left(\frac{1.2 \text{ kHz}}{\nu_{\text{K}}} \right)^2 . \quad (13)$$

Computations of the *maximum* values of $I_{45}M_{\odot}/M$ for modern neutron star equations of state are very close to unity. For example, for the FPS equation of state the maximum value of $I_{45}M_{\odot}/M$ is 0.87 and occurs for a $1.55M_{\odot}$ star; for the UU equation of state the maximum is 1.05 and occurs for a $2.1M_{\odot}$ star (M. C. Miller, personal communication). Even for the obsolete and unrealistically stiff equations of state L and M, the maximum values of $I_{45}M_{\odot}/M$ are $\lesssim 2$.

These results show that the frequencies of the bumps seen in the power spectra of the atoll sources are about twice as high as the highest precession frequencies predicted by modern neutron star models, as Stella & Vietri themselves noted. Hence, in order to explain the bumps in the atoll source power spectra by gravitomagnetic precession of the inner disk, the precessing HFGM corrugation would have to generate X-ray brightness oscillations with a frequency equal to twice the precession frequency (i.e., at the second harmonic) or I_{45}/M for these neutron stars would have to be twice as large as the largest values given by modern neutron star equations of state.

The maximum frequencies of the horizontal branch QPOs are $\sim 50\%$ higher than the maximum frequencies of the bumps in the atoll source power spectra and are therefore a factor ~ 3 higher than the highest precession frequencies predicted by modern neutron star equations of state, as Stella & Vietri also noted. For a detailed comparison of all the available data on the atoll sources with the predictions of the gravitomagnetic precession model, see Psaltis et al. (1998).

In addition to resolving whether the frequencies predicted by the gravitomagnetic precession model can be reconciled with the frequencies of the features observed in the power spectra of neutron stars and black hole candidates, the excitation, damping, and visibility in X-rays of the low-order HFGM modes will have to be explored further before they can be regarded as a promising explanation for these features.

Our results show that these modes are not excited by the radiation-warping torque. The two lowest-order HFGM precession modes involve vertical motions of the inner edge of the disk. This offers a possible way of exciting them. In order to excite steadily either of these two modes, a torque acting on the inner edge of the disk would have to match the variation of their phases with azimuth as well as their frequencies. On the other hand, coupling of the vertical motion to the radiation field, magnetic field, or surface of a neutron star may instead damp these modes.

The two lowest HFGM modes might also be excited by repetitive impulsive disturbance of the inner disk. If, however, such disturbances affect the inner portion of the disk as well as its innermost edge, they may excite the broad spectrum of underdamped HFGM modes, rather than one or two such modes, producing a broad spectrum rather than a QPO. Resonant excitation of the $m > 2$ HFGM modes appears difficult, because they do not disturb the inner edge of the disk. In order to excite these modes steadily, the driving force would have to match closely the extremely rapid variation of their phases with radius and azimuth, as well as their frequencies.

The highest-order HFGM modes do not appear promising as a mechanism for producing quasi-periodic oscillations in X-ray brightness, because they are very tightly wound spiral corrugations within a narrow annulus centered at a radius ~ 5 times larger than the radius of the inner edge of the accretion disk and do not affect the accretion disk at its inner edge. On their face, the lowest-order HFGM modes appear more capable of causing oscillations in the X-ray emission, for example by modulating the accretion onto the compact object.

A more complete exploration of the detailed properties of the high-order radiation-warping modes, LFGM modes, LFGMR modes, and HFGM modes will be presented elsewhere.

We are grateful to Philip Maloney, Cole Miller, and Dimitrios Psaltis for many helpful comments, and to Cole Miller for computing the moments of inertia used in § 4. This work was supported in part by NSF grants AST 93-15133 and AST 96-18524 and by NASA grant NAG 5-2925.

REFERENCES

- Bardeen, J. M., & Petterson, J. A. 1975, *ApJ*, 195, L65
- Cui, W., Zhang, S. N., & Chen, W. 1997, *ApJ*, 492, L53
- Hatchett, S. P., Begelman, M. C., & Sarazin, C. L. 1981, *ApJ*, 247, 677
- Iping, R. C., & Petterson, J. A. 1990, *A&A*, 239, 221
- Ipsier, J. R. 1996, *ApJ*, 458, 508
- Kato, S. & Honma, F. 1991. *Publ. Astr. Soc. Japan*, 43, 95
- Lamb, F. K., Shibasaki, N., Alpar, M. A., & Shaham, J. 1985, *Nature*, 317, 681
- Maloney, P. R., & Begelman, M. C. 1997, *ApJ*, 491, L43
- Maloney, P. R., Begelman, M. C., & Nowak, M. A. 1998, *ApJ*, to be published, astro-ph/9803238
- Maloney, P. R., Begelman, M. C., & Pringle, J. E. 1996, *ApJ*, 472, 582
- Miller, M. C., & Lamb, F. K. 1996, *ApJ*, 470, 1033
- Miller, M. C., Lamb, F. K., & Psaltis, D. 1998, *ApJ*, in press
- Miyamoto, S., Kimura, K., Kitamoto, S., Dotani, T., & Ebisawa, K. 1991, *ApJ*, 383, 784
- Morgan, E., Remillard, R., & Greiner, J. 1997, *ApJ*, in press
- Nowak, M. A. & Wagoner, R. V. 1991, *ApJ*, 387, 656
- Papaloizou, J. C. B., & Pringle, J. E. 1983, *MNRAS*, 202, 1181
- Petterson, J. A. 1977a, *ApJ*, 214, 550
- . 1977b, *ApJ*, 216, 827
- . 1978, *ApJ*, 226, 253
- Press, W. H., Teukolsky, S. A., Vetterling, W. T., & Flannery, B. P. 1992, *Numerical Recipes* (Cambridge University Press)
- Pringle, J. E. 1996, *MNRAS*, 281, 357
- Psaltis, D., et al. 1998, *ApJ*, submitted
- Remillard, R. 1997, in *Proc. 18th Texas Symposium on Relativistic Astrophysics*, ed. A. Olinto, J. Friedman, & D. Schramm (World Scientific), in press
- Stella, L. 1997a, talk presented at the Symposium on The Active X-ray Sky: Results from BeppoSAX

and Rossi-XTE, Accademia dei Lincei, Rome, October 1997

———. 1997b, talk presented at the meeting of the High Energy Astrophysics Division of the AAS, Estes Park, Colorado, November 1997

Stella, L., & Vietri, M. 1998, *ApJ*, 492, L59

van der Klis, M. 1995, in *X-Ray Binaries*, ed. W.H.G. Lewin, J. van Paradijs, & E.P.J. van den Heuvel (Cambridge Univ. Press), 252